Computers and Concrete, *Vol. 18, No. 6 (2016) 1065-1082*
DOI: http://dx.doi.org/10.12989/cac.2016.18.6.1065

Modeling mechanical strength of self–compacting mortar containing nanoparticles using wavelet–based support vector machine

Mohsen Khatibinia[*1], Abdosattar Feizbakhsh[1a], Ehsan Mohseni[2b] and Malek Mohammad Ranjbar[2c]

[1]*Department of Civil Engineering, University of Birjand, Birjand, Iran*
[2]*Department of Civil Engineering, University of Guilan, Rasht, Iran*

(Received April 4, 2016, Revised September 2, 2016, Accepted September 10, 2016)

Abstract. The main aim of this study is to predict the compressive and flexural strengths of self–compacting mortar (SCM) containing nano–SiO_2, nano–Fe_2O_3 and nano–CuO using wavelet–based weighted least squares–support vector machines (WLS–SVM) approach which is called WWLS–SVM. The WWLS–SVM regression model is a relatively new metamodel has been successfully introduced as an excellent machine learning algorithm to engineering problems and has yielded encouraging results. In order to achieve the aim of this study, first, the WLS–SVM and WWLS–SVM models are developed based on a database. In the database, nine variables which consist of cement, sand, NS, NF, NC, superplasticizer dosage, slump flow diameter and V–funnel flow time are considered as the input parameters of the models. The compressive and flexural strengths of SCM are also chosen as the output parameters of the models. Finally, a statistical analysis is performed to demonstrate the generality performance of the models for predicting the compressive and flexural strengths. The numerical results show that both of these metamodels have good performance in the desirable accuracy and applicability. Furthermore, by adopting these predicting metamodels, the considerable cost and time–consuming laboratory tests can be eliminated.

Keywords: model mortar; compressive strength; flexural strength; nanoparticles; weighted least squares support vector machine; wavelet

1. Introduction

Mechanical assessment of concrete strengths has been widely considered as the main and most important property of concrete, which is often measured after a standard curing time. The mechanical strength consists of the compressive and flexural strengths which depends on many factors. Other concrete properties such as elastic modulus and water absorption appear to have

[*]Corresponding author, Assistant Professor, E-mail: m.khatibinia@birjand.ac.ir
[a]M.Sc Graduated, E-mail: a.s.feizbakhsh@gmail.com
[b]M.Sc Graduated, E-mail: ehsan.mohseni172@gmail.com
[c]Assistant Professor, E-mail: ranjbar@guilan.ac.ir

http://www.techno-press.org/?journal=cac&subpage=8 ISSN: 1598-8198 (Print), 1598-818X (Online)

direct relationships with the compressive strength. Furthermore, the compressive strength is usually utilized as the major criterion in the evaluation of the concrete quality. Therefore, an accurate estimation of the compressive strength before the use of concrete in constructing engineering projects is very important.

Recently, self-compacting concrete (SCC) has been widely developed and known as a new type of concrete technology (Oltulu and Sahin 2010). Due to the ability to be compacted by its own weight without the need of vibration, the uses of SCC have been increased rapidly in the last three decades (Jalal *et al*. 2012, Madandoust *et al*. 2012). Previous studies were shown that mechanical properties of self–compacting mortar (SCM) are similar to the results of the SCC. Consequently, conducting research on the mortar is more controllable (Niknam and Mousavi 2010). Furthermore, the mechanical properties of SCM can be used to examine and estimate the performance of SCC.

Recently, nanotechnology has widely received the considerable attention due to the new potential use of the nano materials in nanoscale, which can improve the properties of cementitious materials. Nanoparticles (NP) can affect the acceleration of cement hydration, because of their high activity, and also the particles can act as a nano–filler due to their high surface. Hence, the materials efficiently improve compacting the microstructure, reduce the porosity and consequently increase the strength. According to the author's knowledge, several works incorporate nanoparticles into SCM have been done. The most of them have focused on nano–SiO_2 (NS) in cement–based materials (Sobolev *et al*. 2009, Nazari and Riahi 2011a, Oltulu and Sahin 2013, Mohseni *et al*. 2015). Nanoparticles same as other factors like age of curing, water–to–cement ratio and aggregate type can mainly affect the properties of concrete specially strength.

In the last decade, predicting the compressive strength of concrete has been an attractive research, and different approaches have been introduced to estimate the compressive strength based on the mix proportions of different ingredients (Yeh 1998). Various studies have applied artificial intelligence (AI) techniques to predict the compressive strength of SCS (Yeh 1998, Chou *et al*. 2011, Erdal *et al*. 2013). According to previous studies, the AI techniques have proved their superior capability over traditional modelling methods. The successful application of Artificial Neural Network (ANN) as one of AI techniques has been reported for prediction of the compressive strength of concrete (Guang and Zong 2000, Kewalramani and Gupta 2006, Oztaas *et al*. 2005). Although, ANN has the following limitations:

• ANN cannot provide the information about the relative significance of the various parameters (Park and Rilett 1999).

• A common criticism of neural networks is that they require a large diversity of training for operation. The knowledge acquired during training the model is stored in an implicit manner. Thus, it is hard to come up with a reasonable interpretation of the overall structure of the network (Kecman 2001).

• ANN has some intrinsic disadvantages such as slow convergence speed, less generalizing effectiveness, arriving at local minimum and over–fitting problems (Ravi 2008).

The support vector machine (SVM) is a relatively new AI technique which has been widely applied in engineering problems and has yielded encouraging results. The results show that the SVM approach has comparable or higher performance than traditional learning machines and has been utilized as a powerful tool to solve classification and regression problems (Chou *et al*. 2011, Cevik *et al*. 2015). However, the SVM approach consists of several inherent drawbacks. Firstly, the approach is unable to provide high prediction accuracy for either the penalty parameter or kernel parameter settings. Secondly, it considers all training data points equally in order to construct the decision surface. Hence, Suykens *et al*. (2002) introduced weighted least squares–

support vector machines (WLS–SVM) as a machine learning algorithm that keeps the estimate more robust and precise by assigning weights for training samples. Over the past few years, WLS–SVM has been applied in many engineering problems successfully (Quan *et al*. 2010, Sobhani *et al.* 2013, Khatibinia and Khosravi 2014, Mirzaei *et al*. 2015, Mahani *et al*. 2015, Katibinia *et al*. 2016, Chitti *et al*. 2016). Recently, a combination of WLS–SVM and Morlet wavelet kernel function, called WWLS–SVM has been introduced (Khatibinia *et al*. 2013a, b, Gharehbaghi and Khatibinia 2015). The results have demonstrated that the wavelet kernel function effectively improve the performance of WLS–SVM.

The main purpose of this study is to predict the compressive and flexural strengths of SCMs incorporating different types of NPs based on using the WLS–SVM and WWLS–SVM models. Although, the superiority of the SVM approaches have been strongly indicated in various recent applications, none of the previous research has investigated the capability of the WWLS–SVM and WWLS–SVM models for predicting the SCM strength. Hence, the main aims of this study are:

• Develop the reliable and robust WWLS–SVM and WLS–SVM models for predicting the mechanical properties of SCM.

• Explore the influence of wavelet and Gaussian radial basis function (RBF) kernel functions on the performance of the WLS–SVM model.

• Compare the results of WWLS–SVM and WLS–SVM with those of other techniques.

2. Experimental program

2.1 Material

Ordinary Portland Cement (OPC) type II and natural river sand were used conforming to ASTM C150 (2001) and ASTM C778 (2011), respectively. According to the ASTM standard, fly ash (FA) as an additive material can be used to improve the workability of SCMs. The physical properties and chemical composition of cement and FA are given in Table 1.

Table 1 The chemical composition and physical properties of cement and FA

Chemical analysis		
Constituents (%)	Cement	FA
SiO_2	21.75	55.8
Al_2O_3	5.15	20.75
Fe_2O_3	3.23	6.66
CaO	63.75	4.12
MgO	1.15	1.9
SO_3	1.95	0.44
K_2O	0.56	1.73
Na_2O	0.33	0.78
L.O.I	2.08	1.95
Physical properties		
Surface area (m^2/g)	0.32	0.28
Specific gravity (g/cm^3)	3.15	2.2

Table 2 Properties of nanoparticels

Nanoparticles	Average Diameter (*nm*)	Specific Surface Area (m^2/g)	Purity (%)
Nano SiO_2	15	200	> 99
Nano Fe_2O_3	60	60	> 98
Nano CuO	15	200	> 99

In Table 1, the nanoparticles include nano SiO_2, nanoCuO and nano Fe_2O_3 with an average particle size of 20 *nm* which is used as a partial replacement for cement. Some properties of these nanoparticles are shown in Table 2.

2.2 Mixture proportions

A total of 22 mixture specimens were produced with having constant water/binder ratio of 0.4 and total binder of 700 kg/m^3. The amount of FA was 25wt.% of the cement. The proportion of the nanoparticles amount used were determined at rations corresponding to 1, 3 and 5wt.% of the binder. The amounts of FA and NPs were considered by carrying out a number of preliminary trials.

In this study, the label of NS, NF and NC denote the SCMs containing nano–SiO_2, nano–Fe_2O_3 and nano–CuO, respectively. The number before the letter N indicates the amount of NPs were added in the mortar. For example, 3NS mortar mixture is consisted of nano–SiO_2 at ratio of 3wt%. The overall proportion of NPs in the single, binary and ternary mixing was identical. For example, in binary combinations containing 1% nanoparticles, each amount of nanoparticle was obtained with a ratio of 1%/3. For example, the 1NSC mortar consists of 1%/2 nano–SiO_2 and 1%/2 nano–CuO. In order to achieve the desired flow ability of the mixtures, a polycarboxylate type super plasticizer (SP) conforming to ASTM C494 type F, with a density of 1.03 g/cm^3 was utilized. The amount of SP was varied to satisfy slump flow diameter and V–funnel flow time, according to the standards of the EFNARC committee (2002). The mix proportions of the SCMs are given in Table 3.

2.3 Test procedure

Since NPs may not show a uniform distribution in the mixture due to their large surface area, it directly influences on the physical and mechanical properties of mortars. In the present study, after several pioneer experiments was finalized according to:

First, the cement and sand were dry mixed in the mixer at a moderate speed for approximately 60*sec*. Then, FA and 30% of the mixing water inclusive NPs were added at high speed for 60 seconds. The mixture was allowed to rest for around 90 *sec*. And finally, SP and remain of the water (70%) were added and mixed for 120 *sec*.

When the mixing was completed, slump flow and V–funnel tests were conducted on the fresh mortars in accordance with the procedure recommended by the EFNARC committee. Any bleeding or segregation of the mortars was observed visually.

Fresh mortar was cast into 50×50×50 *mm* cubes for compressive strength, and into 50×50×200 *mm* prismatic moulds for flexural strength. After one day, the specimens were placed in water at

Table 3 Mixture proportions of the mortars

Label	Cement (kg/m^3)	FA (kg/m^3)	Nano SiO_2 (kg/m^3)	Nano Fe_2O_3 (kg/m^3)	Nano CuO (kg/m^3)	Water (kg/m^3)	Sand (kg/m^3)	SP (kg/m^3)
Control	525	175	0	0	0	280	1210	4.5
1NS	518	175	7	0	0	280	1198	4.5
3NS	504	175	21	0	0	280	1176	4.2
5NS	490	175	35	0	0	280	1153	4.2
1NF	518	175	0	7	0	280	1198	4.2
3NF	504	175	0	21	0	280	1176	4
5NF	490	175	0	35	0	280	1153	4
1NC	518	175	0	0	7	280	1198	4.2
3NC	504	175	0	0	21	280	1176	4
5NC	490	175	0	0	35	280	1153	3.9
1NSF	518	175	3.5	3.5	0	280	1198	4.2
3NSF	504	175	10.5	10.5	0	280	1176	4.2
5NSF	490	175	17.5	17.5	0	280	1153	4
1NSC	518	175	3.5	0	3.5	280	1198	4.1
3NSC	504	175	10.5	0	10.5	280	1176	4
5NSC	490	175	17.5	0	17.5	280	1153	4
1NFC	518	175	0	3.5	3.5	280	1198	4
3NFC	504	175	0	10.5	10.5	280	1176	3.8
5NFC	490	175	0	17.5	17.5	280	1153	3.8
1NSFC	518	175	2.3	2.3	2.3	280	1198	3.8
3NSFC	504	175	7	7	7	280	1176	3.8
5NSFC	490	175	11.7	11.7	11.7	280	1153	3.5

$21\pm2\ ^{\circ}C$ until testing. Mechanical properties of hardened mortars consist of the compressive and flexural strength were measured at 3, 7, 28 and 90 days. Afterward the average of three specimens were assigned to each specimens.

3. Experimental result

3.1 Properties of fresh self-compacting mortar

Table 4 shows the rheological test results containing slump flow diameter and V–funnel flow time. All of mixtures were designed to have a slump flow diameter of $25\pm1\ cm$ which achieved by using the desirable dosage of SP. The mini V–funnel flow times were in range of 7.7–11 seconds. The highest mini V–funnel flow time measured for the control sample and the 5NC mix shows the lowest flow time of V–funnel test.

Table 4 Fresh properties of SCMs

Label	Slump flow diameter (*cm*)	V–funnel flow time (*sec*)
Control	24.5	11
1NS	24.5	10.2
3NS	24.8	9.7
5NS	25	8.3
1NF	24.7	10.8
3NF	24.9	9.8
5NF	25.5	7.6
1NC	24.5	9.8
3NC	24.8	8.2
5NC	25.5	7.7
1NSF	24.5	10.1
3NSF	24.9	9.8
5NSF	25	9.5
1NSC	24.5	10.5
3NSC	25.2	9.1
5NSC	25.5	7.7
1NFC	24.3	10.9
3NFC	24.5	10.7
5NFC	24.6	9.9
1NSFC	24.5	10.5
3NSFC	24.6	9.9
5NSFC	25	8.7

3.2 Mechanical properties of self–compacting mortar

3.2.1 Compressive strength

The results of the compressive strength are shown in Fig. 1. As can be seen from Fig. 1, the compressive strength is improved in all ages except for the combination containing NF in early ages (i.e. 3 and 7 days). This may be due to pozzolanic activity of the samples of FA and NF. Another possible reason can be in the virtue of excessive amount of NF for the sake of bigger size of NF that decrease the filler effect of NPs. The samples incorporating NC demonstrates the most improvement in the compressive strength. The comparison with the single mixtures containing 3NC shows the highest compressive strength, that improves the strength up to 20%. This result is in agreement with work of Nazari and Riahi (2011b), which can be related to acceleration of the calcium–silicate–hydrate (C–S–H) gel.

Among all mixtures, the combination of NS+NC indicates the best improvement in the compressive strength of specimens containing NPs in binary combinations. The 5NSC sample also gives the greatest enhancement which is around 30% at all ages. In binary mixtures the results show that the reduction of strength is occurred after addition of 3wt% NPs, except for NSC. It is due to the weak pore structure of SCMs, decreasing the C–S–H gel, consequently having the weak

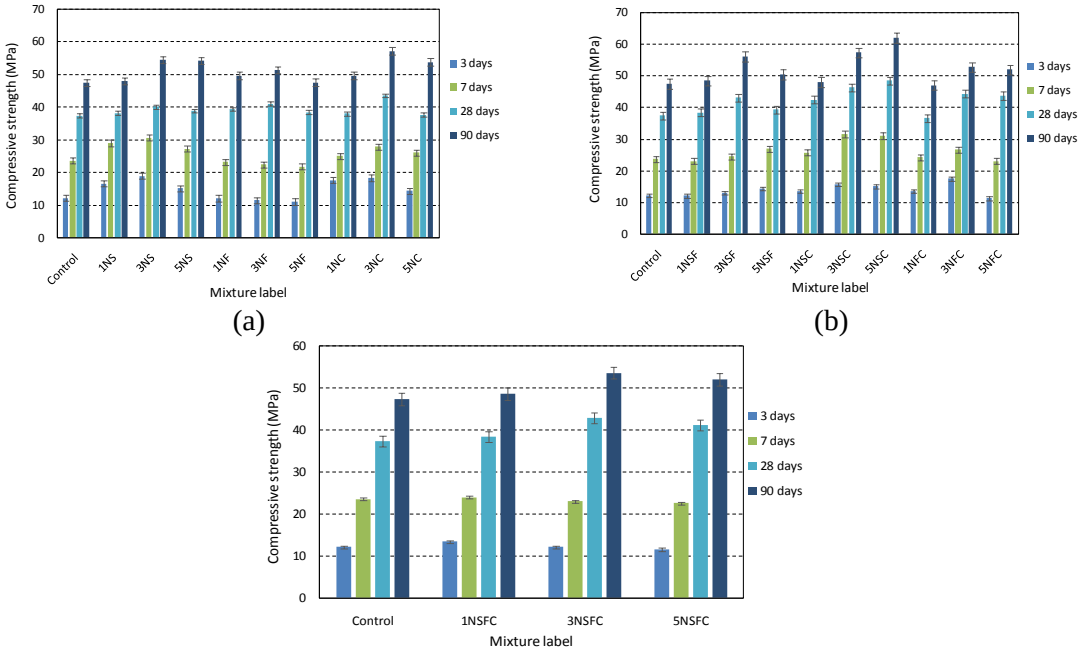

Fig. 1 Compressive strength of self–compacting mortar mixture containing (a)single, (b)binary and (c)ternary dosage of NPs

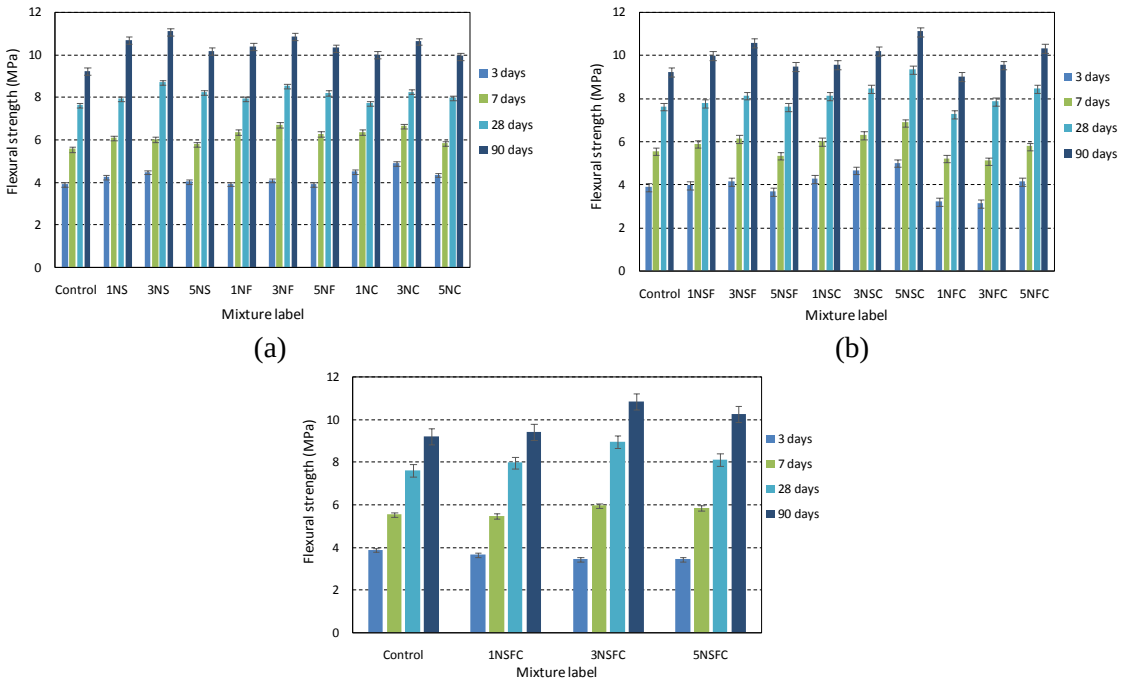

Fig. 2 Flexural strength of self–compacting mortar mixture containing (a)single, (b)binary and (c) ternary dosage of NPs

microstructure of cement matrix. In ternary combination of NPs the compressive strength is decreased at early ages, although it is observably increased at older ages.

3.2.2 Flexural strength

The results of the flexural strength of SCMs containing NPs are depicted in Fig. 2. It can be seen from Fig. 2 that the single NPs in comparison with the control sample improves the flexural strength, although in some binary and ternary mixtures of NPs some drawbacks are observed. In the mixtures containing single NPs, the addition of 3% could be the best percentage.

Using the comparison of the results, the binary mixtures had different trends. First of all, the combination of NS and NC, for instance of 5NSC sample, the flexural strength showed an increase of about 16–30%, which is due to pozzolanic action and filler effect. By adding NS+NF, different trend can be seen. Addition of 1 and 3% increased the flexural strength and after that decreased. Finally, the combination of NF and NC showed reduction in early ages and improvement in older ages. The ternary combination of NPs, showed reduction by adding 1%. Also, 3% replacement of nanoparticles is the most desirable percentage by about 19% improvement in flexural strength.

4. Wavelet kernel function–based metamodel

4.1 Least squares support vector machine

Support vector machines (SVMs) proposed by Vapnik and Lerner (1963) have strong theoretical foundation for modeling the high non–linear system based on small sample. The SVMs approaches have been developed based on the structural risk minimization (SRM) rules which can avoid the problems of over learning, dimension disaster and local minimum. This metamodel has been utilized in many classification andregression problems successfully (Park and Ang 1985). The least squares support vector machine (LS–SVM) presented by Suykens *et al*. (1999) overcome the drawbacks of SVM such as slow training velocity in the large–scaleproblem.

Consider a set of training data $\{(x_1,y_1),\ldots,(x_n,y_n)\} \subset \boldsymbol{X}$, where $\boldsymbol{X}$ denotes the space of input patterns. In the modeling of LS–SVM regression, the error ξ_i quadratic norm is taken as the loss function of LS–SVM. The optimization problem is described as follows (Suykens *et al*. 1999)

$$\min J(\boldsymbol{\omega},\xi) = \frac{1}{2}\|\boldsymbol{\omega}\|^2 + \frac{1}{2}C\sum_{i=1}^{n}\xi_i^2 \tag{1}$$

subject to the equality restriction

$$y_i = \boldsymbol{\omega}^T\varphi(\boldsymbol{x}_i) + b + \xi_i, \qquad i = 1,2,...,n \tag{2}$$

Therefore, the model of the LS–SVM regression is defined as follows

$$y(\boldsymbol{x}) = \boldsymbol{\omega}^T\phi(\boldsymbol{x}) + b \tag{3}$$

In Eq. (1), C defined as punishment factor determines the tradeoff between the complexity of the LS–SVM model, i.e. $y(\boldsymbol{x})$, and its accuracy in capturing the training data. The LS–SVM's loss function is different from the standard SVM. For the optimization problem, the Lagrange function is introduced as follows

$$L(\boldsymbol{\omega},b,\xi,\boldsymbol{\alpha})=\frac{1}{2}\|\boldsymbol{\omega}\|^2+C\sum_{i=1}^{n}\xi_i^2-\sum_{i=1}^{n}\alpha_i[\boldsymbol{\omega}^T\varphi(x_i)+b+\xi_i-y_i] \tag{4}$$

In Eq. (4), α_i (i=1,2,…,n) are the Lagrange multiplier. Based on the Karush–Khun–Tucker (KKT) conditions, by eliminating $\boldsymbol{\omega}$, $\boldsymbol{\xi}$ the solution is given by the following set of linear equation

$$\begin{bmatrix} 0 & 1 & \cdots & 1 \\ 1 & K(x_1,x_1)+\frac{1}{C} & \cdots & K(x_1,x_n) \\ \vdots & \vdots & \vdots & \vdots \\ 1 & K(x_1,x_n) & \cdots & K(x_n,x_n)+\frac{1}{C} \end{bmatrix}\begin{bmatrix} b \\ \boldsymbol{\alpha} \end{bmatrix}=\begin{bmatrix} 0 \\ y_1 \\ \vdots \\ y_n \end{bmatrix} \tag{5}$$

where $K(.,.)$ is so–called kernel function. According to Mercer's condition, a kernel $K(.,.)$ is selected, such that

$$K(\mathbf{x},\bar{\mathbf{x}})=\langle\phi(\mathbf{x}),\phi(\bar{\mathbf{x}})\rangle_H \tag{6}$$

In fact, $K(\square,\square)$ describes the high dimensional feature spaces that is non–linearly mapped from the input space x. Thus, the following LSSVM model is concluded as follows:

$$y(\boldsymbol{x})=\sum_{i=1}^{n}\alpha_i K(\boldsymbol{x},x_i)+b \tag{7}$$

4.2 Weighted least squares–support vector machine

Due to assigning weights in the weighted least squares–support vector machine (WLS–SVM), WLS–SVM in comparison with LS–SVM can predict functions in a more robust and precise manner. It is shown that the performance of WLS–SVM is better than the LS–SVM (Suykens *et al*. 2002). In order to achieve this purpose, the error ξ is weighted. Therefore, the WLS–SVM model is presented as the following optimization problem in primal weight space (Quan *et al*. 2010)

$$\min J(\boldsymbol{\omega},\xi)=\frac{1}{2}\|\boldsymbol{\omega}\|^2+\frac{1}{2}C\sum_{i=1}^{n}v_i\xi_i^2 \tag{8}$$

and the constrain of WLS–SVM is Eq. (2). It is impossible to indirectly calculate $\boldsymbol{w}$ from Eq. (8), because the structure of the function $\varphi(\boldsymbol{x})$ is unknown. Hence, the dual problem described in Eq. (8) is minimized by the Lagrange multiplier concept as follows

$$L(\boldsymbol{\omega},b,\xi,\boldsymbol{x})=J(\boldsymbol{\omega},\xi)-\sum_{i=1}^{n}\alpha_i(\boldsymbol{\omega}^T\varphi(\boldsymbol{x}_i)+b+\xi_i-y_i) \tag{9}$$

Based on the KKT conditions, by eliminating $\boldsymbol{\omega}$ and ξ the solution is given by the following set of linear equations

$$\begin{bmatrix} \Omega + \boldsymbol{V}_{\gamma} & \boldsymbol{1}_n^T \\ \boldsymbol{1}_n & \boldsymbol{0} \end{bmatrix} \begin{bmatrix} \boldsymbol{\alpha} \\ b \end{bmatrix} = \begin{bmatrix} \boldsymbol{y} \\ 0 \end{bmatrix} \tag{10}$$

where

$$\begin{gathered} \boldsymbol{V}_{\gamma} = diag\{1/Cv_1,...,1/Cv_n\} \; ; \; \Omega_{i,j} = \left\langle \varphi(\boldsymbol{x}_i), \varphi(\boldsymbol{x}_j) \right\rangle_H \quad i, j = 1,...,n \\ \boldsymbol{y} = [y_1,...,y_n]^T ; \; \boldsymbol{1}_n^T = [1,...,1] \; ; \; \boldsymbol{\alpha} = [\alpha_1,...,\alpha_n] \end{gathered} \tag{11}$$

So, the WLS–SVM model same as LS–SVM can be provided for the prediction of functions, which defined in Eq. (7). After weights v_k are determined, the model defined in Eq. (7) is obtained after solving the WLS–SVM problem (i.e. Eq. (10)). In the WLS–SVM models, the Gaussian radial basis function (RBF) as the kernel function is applied and expressed as

$$K(\boldsymbol{x}, \bar{\boldsymbol{x}}) = \exp\left(-\frac{\left\| \boldsymbol{x} - \bar{\boldsymbol{x}} \right\|^2}{\sigma^2}\right) \tag{12}$$

where σ^2 is a positive real constant, and it is usually called the kernel width.

4.3 Wavelet kernel–based WLS–SVM

Wavelet kernel–based SVMs have been proposed and widely developed in many applications (Wu 2010, Wu 2011, Calisir and Dogantekin 2011, Zavar *et al*. 2011). The wavelet functions as kernel function can effectively improve the performance of the SVM approaches. A function $\psi \in L^2(\boldsymbol{R})$ as a wavelet is introduced if it has zero average on (Lekutai 1997)

$$\int_{-\infty}^{+\infty} \psi(x)\, dx = 0 \tag{13}$$

Morlet's basic wavelet function as the mother wavelet has be proposed by multiplying of the Fourier basis with a Gaussian window (Martinet *et al*. 1987). Khatibinia *et al*. (2013a, b) introduced a wavelet kernel–based WLS–SVM that employ the cosine–Gaussian Morlet wavelet with $\omega_0 = 4$ as the kernel function of WLS–SVM. The wavelet function is expressed as follows

$$\psi(x) = \frac{1}{\sqrt{a}} \cos\left[\omega_0 \left(\frac{x-c}{a}\right) \right] \exp\left[-0.5 \left(\frac{x-c}{a}\right)^2 \right] \tag{14}$$

Hence, the wavelet kernel function can be defined as (Martinet *et al*. 1987)

$$K(\boldsymbol{x}, \bar{\boldsymbol{x}}) = \prod_{i=1}^{n} \psi\left(\frac{\boldsymbol{x}_i - c_i}{a}\right) \psi\left(\frac{\bar{\boldsymbol{x}}_i - \bar{c}_i}{a}\right) \tag{15}$$

where *n* is the number of samples; $\boldsymbol{x}$ and $\bar{\boldsymbol{x}} \in \boldsymbol{R}^n$, and Eq. (16) is called as dot–product wavelet kernels. Thus, the translation–invariant wavelet kernel can be explained as follows

$$K(\boldsymbol{x}, \bar{\boldsymbol{x}}) = \prod_{i=1}^{n} \psi\left(\frac{\boldsymbol{x}_i - \bar{\boldsymbol{x}}_i}{a}\right) \tag{16}$$

According to Eqs. (14) and (16), the wavelet kernel function of the cosine–Gaussian Morlet wavelet is obtained as follows

$$K(\boldsymbol{x},\bar{\boldsymbol{x}})=\prod_{i=1}^{n}\frac{1}{\sqrt{a}}\cos\left[\omega_0\left(\frac{\boldsymbol{x}_i-\bar{\boldsymbol{x}}_i}{a}\right)\right]\exp\left(-0.5\frac{\left\|\boldsymbol{x}_i-\bar{\boldsymbol{x}}_i\right\|}{a^2}\right) \tag{17}$$

In the work of Khatibinia *et al*. (2013a), it has been shown that the best performance of WWLS–SVM was obtained with a=6.75. The general structure of the WLS–SVM and WWLS–SVM models is depicted in Fig. 3:

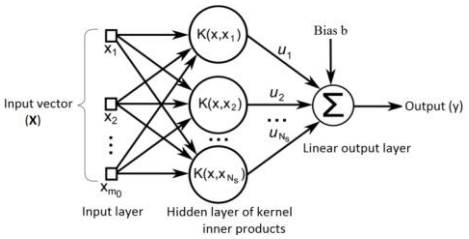

Fig. 3 The general structure of the WWLS–SVM and WLS–SVM models (Mirzaei *et al*. 2015)

5. Prediction of the mechanical strengths of SCM

5.1 Development of the metamodel

In this study, a set of 82 samples as database is utilized to develop the WLS–SVM and WWLS–SVM models for predicting the mechanical strength of SCM. Each sample contains cement, sand, NS, NF, NC, superplasticizer dosage, Slump flow diameter and V–funnel flow time as input variables of the database, the compressive and flexural strengths of SCM as the output variables of the database. The data are obtained from the experimental studies. Table 5 shows descriptive statistics for these input variables and the outputs.

Table 5 Statistical description of mortar components

Factors	Unit	Min	Max	Mean	Standard deviation	Skewness	Kurtosis
Cement	kg/m^3	490	525.0	504.95	12.28	0.01	–1.49
Nano SiO_2	kg/m^3	0.00	35.00	6.68	9.21	1.69	2.99
Nano Fe_2O_3	kg/m^3	0.00	35.00	6.68	9.21	1.69	2.99
Nano CuO	kg/m^3	0.00	35.00	6.68	9.21	1.69	2.99
Sand	kg/m^3	1153	1210	1177.23	19.78	–0.01	–1.46
SP	kg/m^3	3.50	4.50	4.04	0.23	0.00	0.70
Slump flow diameter	*cm*	24.3	25.50	24.81	0.36	0.72	–0.42
V–funnel flow time	*sec*	7.60	11.00	9.56	1.09	–0.61	–0.84
Compressive strength	*MPa*	11.00	61.97	33.08	14.82	0.04	–1.33
Flexural strength	*MPa*	3.11	11.10	7.08	2.36	0.04	–1.24

Before scaling dividing database, the values of the input variables are normalized as follows

$$\overline{x}_i = b_1 \frac{x_i - x_{\min}}{x_{\max} - x_{\min}} + b_2 \tag{18}$$

where $\overline{x}_i$, $x_{\max}$ and $x_{\min}$ are the normalized, maximum and minimum values of the input and output variables, respectively. In this study, b_1 and b_2 are assigned the values 0.6 and 0.2, respectively.

To predict the compressive and flexural strengths of SCM, at first, the samples are selected on a random basis and from which 70% and 30% samples are employed to train and test the metamodels. Then, two WLS–SVM and WWLS–SVM models with the 10–fold cross–validation are trained based on the database. Furthermore, a grid search algorithm is employed in the parameter space in order to obtain the optimal model parameters of the metamodels. According to Khatibinia *et al*. (2013a), the WLS–SVM model based on RBF and wavelet kernel functions for predicting of output data is performed using the following procedure:

Step 1: Assign training data $\{\mathbf{x}_k, y_k\}_{k=1}^{Ntot}$, set *N=Ntot*.

Step 2: Find an optimal (γ, σ) combination on the total amount of *Ntot* training data by 10–fold cross–validation, and solve linear system (10), give the model (7).

Step 3: Sort the values $|\boldsymbol{\alpha}|$.

Step 4: Remove a small number of *M* points (typically 5% of the *N* points) that has the smallest values in the sorted $|\boldsymbol{\alpha}|$.

Step 5: Retain *N–M* points and set *N=N–M*.

Step 6: Go to 2 and retrain on the reduced training set.

To investigate the accuracy of the metamodels, the mean absolute percentage error (*MAPE*), the relative root–mean–squared error (*RRMSE*) and the absolute fraction of variance (R^2) are adopted as the performance criteria. The criteria are computed as following (Topcu and Sandemir 2008)

$$MAPE = \frac{1}{n_t} \sum_{i=1}^{n_t} 100 \times \left| \frac{y_i - \overline{y}_i}{y_i} \right| \tag{19}$$

$$RRMSE = \sqrt{\frac{n_t \sum_{i=1}^{n_t} (y_i - \overline{y}_i)^2}{(n_t - 1) \sum_{i=1}^{n_t} y_i^2}} \tag{20}$$

$$R^2 = 1 - \left(\frac{\sum_{i=1}^{n_t} (y_i - \overline{y}_i)^2}{\sum_{i=1}^{n_t} \overline{y}_i^2} \right) \tag{21}$$

where$y$ and $\overline{y}$ are actual value and predicted value, respectively; and n_t is the number of testing samples. The smaller *RRMSE* and *MAPE* and the larger R^2, are the indicative of better performance.

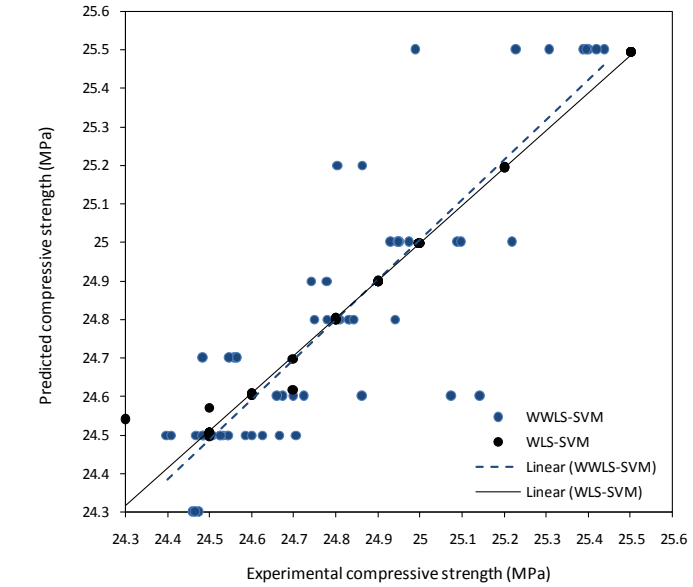

(a) training phase

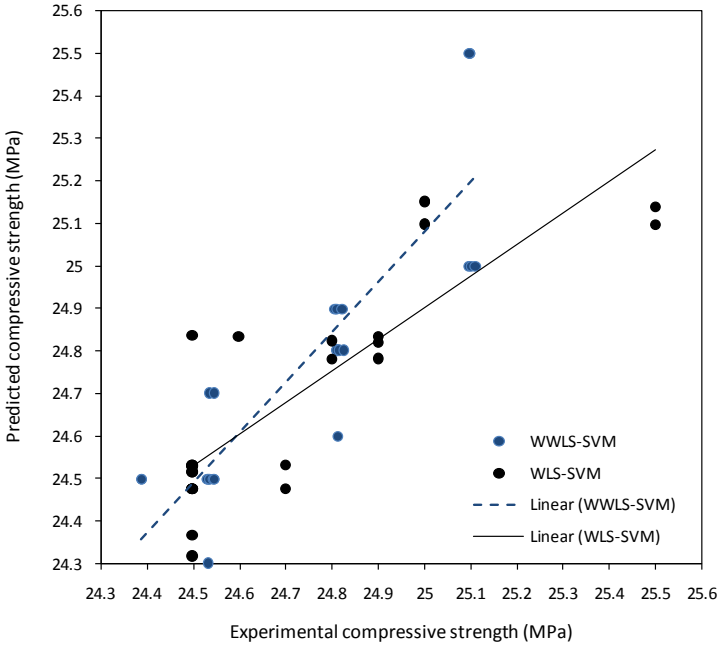

(b) testing phase

Fig. 4 Observed versus predicted the compressive strength for WWLS–SVM and WLS–SVM methods

5.2 Results and discussion

Figs. 4 and 5 show scatter diagrams for the actual and predicted values of training data and testing data, respectively.

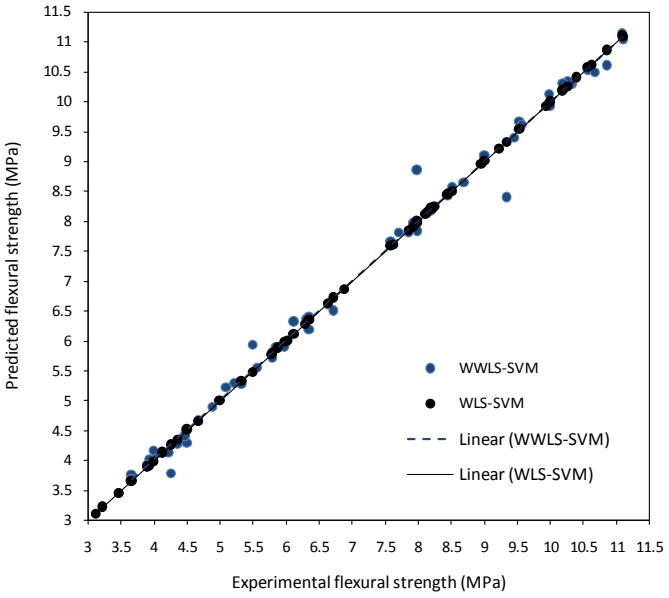

(a) training phase

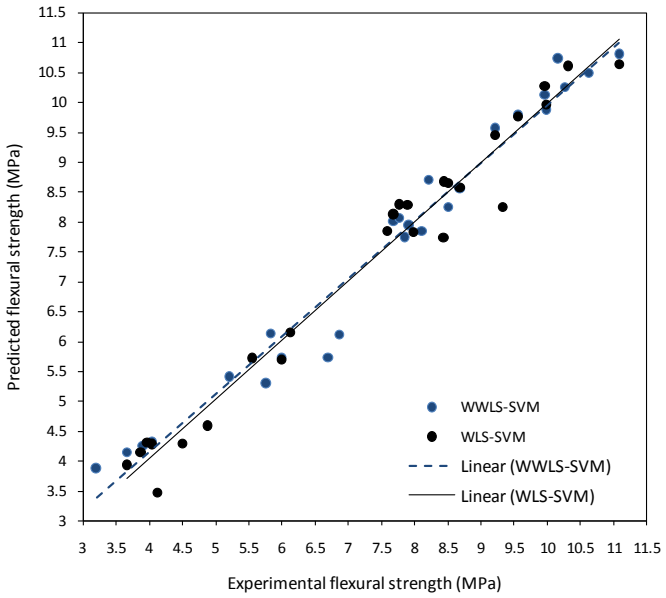

(b) testing phase

Fig. 5 Observed versus predicted the flexural strength for WWLS–SVM and WLS–SVM methods

It is obvious from Figs. 4 and 5 that, visually, the distribution of the compressive and flexural strength data predicted the WLS–SVM and WWLS–SVM models remarkably fit the distribution of the experimental data. The performance generality of the WLS–SVM and WWLS–SVM models based on the statistical value of R^2 are also reported in Table 6 for the compressive strength and flexural strength, respectively.

Table 6 R^2 value for the prediction of the mechanical strength

Mechanical strength	Phase	WWLS–SVM	WLS–SVM
Compressive strength	Train	0.9999	0.9999
	Test	0.9999	0.9999
Flexural strength	Train	0.9999	0.9996
	Test	0.9997	0.9994

It can be seen from Table 6 that the predicted values of the mechanical strengths based on the WLS–SVM and WWLS–SVM models are exactly similar to the experimental values.

5.3 Comparison of results with other techniques

This section presents the results from the comparison of the WLS–SVM and WWLS–SVM models with other prediction techniques including adaptive–network–based fuzzy inference system (ANFIS) and ANN metamodels. The results of the WLS–SVM and WWLS–SVM models were obtained as explained in the previous section. In order to clarify an overall comparison, all statistical criteria used in testing data are combined to create a normalized reference index (*RI*) (Chou *et al*. 2011). For this purpose, at first, each of the performance criteria is normalized to a value of 1 for the best performance and 0 for the worst. Then, the RI is obtained by calculating the average of every normalized performance criteria as shown in Eq. (22).

$$RI = \frac{RRMSE + MAPE}{2} \tag{22}$$

also, Eq. (23) is used for normalizing the performance criteria as

$$f_{norm,i} = \frac{f_{\max,i} - f_i}{f_{\max,i} - f_{\min,i}} \tag{23}$$

Hence, Tables 7 and 8 show the results obtained based on the WLS–SVM, WWLS–SVM ANFIS and ANN techniques for the performance comparison of the metamodels.

Table 7 Performance measurement results of various prediction techniques for the compressive strength

Model	Training phase			Testing phase			
	MAPE	*RRMSE*	R^2	*MAPE*	*RRMSE*	*RI*	R^2
WLS–SVM	0.0365	0.0014	0.9999	0.4632	0.0067	1.000	0.9999
WWLS–SVM	0.4768	0.0069	0.9999	0.4717	0.0069	0.999	0.9999
ANN	10.154	2.2930	0.9947	12.5809	1.7142	0.178	0.9915
ANFIS	11.517	2.6579	0.9895	14.2869	2.2338	0.0	0.9882

Table 8 Performance measurement results of various prediction techniques the flexural strength

Model	Training phase			Testing phase			
	MAPE	*RMSE*	R^2	*MAPE*	*RMSE*	*RI*	R^2
WWLS–SVM	0.8060	0.0103	0.9999	4.8817	0.0528	1.000	0.9996
WLS–SVM	1.2912	0.0250	0.9997	6.3448	0.0570	0.9328	0.9997
ANN	11.235	2.2845	0.9911	14.0357	2.7142	0.1225	0.9899
ANFIS	12.517	2.6684	0.9815	15.8952	2.9338	0.0	0.98100

Based on the *RI* index obtained from testing process, the WLS–SVM and WWLS–SVM models outperformed the ANN and ANFIS techniques. In fact, the WLS–SVM and WWLS–SVM models in comparison with the ANN and ANFIS techniques could accurately predict the compressive and flexural strengths using few samples. Furthermore, the WWLS–SVM metamodel obtained the best result for every performance measure, with an *RI* value of 1.00. Due to the superior performance of the WWLS–SVM model over the other models, the WWLS–SVM model instead of time–consuming laboratory tests can be considered as an the robust approach for predicting the compressive and flexural strengths of SCM.

6. Conclusions

In this study, the weighted least squares–support vector machines (WLS–SVM) approach based on Gaussian radial basis function (RBF) and wavelet kernel functions was utilized to predict the mechanical strength of SCM. The following results could be drawn from this study:

• Incorporation of nanoparticels, whether used single alone, binary and ternary combination except for NF samples in some cases, had an influential effect in compressive and flexural strengths of SCMs. As an average, the most increased related to adding 3NS and NC in single, and 5NSC in binary mixtures at all ages. The results showed that in binary mixtures, incorporation of NS+NC was the best results at both early and older ages. Although the suitable percentages of incorporation was 3 in early and 5 in older ages. However, using ternary combination of NPs didn't result significant influences in early ages, but it caused to improve the mechanical properties at older ages. Due to common results, it was found the best combination to arise the strength was 3% of NPs.

• In order to predict the effects of NPs in SCMs containing fly ash, two different WWLS–SVM and WLS–SVM approach models are proposed. It was observed that these models could effectively be used as a tool to assign the mechanical properties of SCMs.

• The WLS–SVM and WWLS–SVM models in comparison with the ANN and ANFIS techniques can accurately predict the compressive and flexural strengths using few samples.

• The results indicate that the generality performance of the WLS–SVM model based on the wavelet kernel, such as Morlet kernel function, is better than the RBF kernel function in predictive ability and precision.

Therefore, based on the significant results the WWS–SVM and WLS–SVM can be considered as an the robust approach for predicting the compressive and flexural strengths of self–compacting mortar.

References

ASTM C150 (2001), "Standard specification for Portland cement, Annual Book of ASTM Standards", ASTM, Philadelphia, PA, USA.

ASTM C778 (2011), "Standard specification for standard sand, annual book of ASTM standards", ASTM, Philadelphia, PA, USA.

Çalişir, D. and Doğantekin, E. (2011), "An automatic diabetes diagnosis system based on LDA-Wavelet Support Vector Machine Classifier", *Exp. Syst. Appl.*, **38**(7), 8311-8315.

Çevik, A., Kurtoğlu, A.E., Bilgehan, M., Gülşan, M.E. and Albegmprli, H.M. (2015), "Support vector machines in structural engineering: a review", *J. Civil Eng. Manag.*, **21**(3), 261-281.

Chitti, H., Khatibinia, M., Akbarpour, A. and Naseri, H.R. (2016), "Reliability-based design optimization of

concrete gravity dams using subset simulation", *Int. J. Optim. Civil. Eng.*, **6**(3), 329-348.
Chou, J.S., Chiu, C.K., Farfoura, M. and Al-Taharwa, I. (2011), "Optimizing the prediction accuracy of concrete compressive strength based on a comparison of data–mining techniques", *J. Comput. Civ. Eng.*, **25**(3), 242-253.
EFNARC (2002), "Specification and guidelines for self–compacting concrete", UK.
Erdal, H.I., Karakurt, O. and Namli, E. (2013), "High performance concrete compressive strength forecasting using ensemble models based on discrete wavelet transform", *Eng. Appl. Artif. Intell.*, **26**(4), 1246-1254.
Gharehbaghi, S. and Khatibinia, M. (2015), "Optimal seismic design of reinforced concrete structures under time history earthquake loads using an intelligent hybrid algorithm", *Earth. Eng. Eng. Vib.*, **14**(1), 97-109.
Guang, N.H. and Zong, W.J. (2000), "Prediction of compressive strength of concrete by neural networks", *Cement Concrete Res.*, **30**(8), 1245-1250.
Jalal, M., Mansouri, E., Sharifipour, M. and Pouladkhan, A.R. (2012), "Mechanical, rheological, durability and microstructural properties of high performance self-compacting concrete containing SiO_2 micro and nanoparticles", *Mater. Des.*, **34**, 389-400.
Kecman, V. (2001), "Leaming and soft computing: Support vector machines, neural networks, and fuzzy logic models", The MIT Press, Cambridge, Massachusetts, London, England.
Kewalramani, M.A. and Gupta, R. (2006), "Concrete compressive strength prediction using ultrasonic pulse velocity through articial neural networks", *Automat. Constr.*, **15**(3), 374-379.
Khatibinia, M. and Khosravi, S. (2014), "A hybrid approach based on an improved gravitational search algorithm and orthogonal crossover for optimal shape design of concrete gravity dams", *Appl. Soft Comput.*, **16**, 223-233.
Khatibinia, M., Chitti, H., Akbarpour, A. and Naseri, H.R. (2016), "Shape optimization of concrete gravity dams considering dam–water–foundation interaction and nonlinear effects", *Int. J. Optim. Civil. Eng.*, **6**(1), 115-34.
Khatibinia, M., Fadaee, M.J., Salajegheh, J. and Salajegheh, E. (2013), "Seismic reliability assessment of RC structures including soil–structure interaction using wavelet weighted least squares support vector machine", *Reliability Eng. Syst. Safety*, **110**, 22-33.
Khatibinia, M., Gharehbagh, S. and Moustafa, A. (2015), "Seismic reliability-based design optimization of reinforced concrete structures including Soil-Structure interaction effects", *Earthquake Engineering–From Engineering Seismology to Optimal Seismic Design of Engineering Structure*, 267-304.
Khatibinia, M., Salajegheh, E., Salajegheh, J. and Fadaee, M.J. (2013b), "Reliability-based design optimization of RC structures including soil–structure interaction using a discrete gravitational search algorithm and a proposed metamodel", *Eng. Optimiz.*, **45**(10), 1147-1165.
Kronland-Martinet, R., Morlet, J. and Grossmann, A. (1987), "Analysis of sound patterns through wavelet transforms", *Int. J. Pattern Recogn. Artif. Intell.*, **1**(02), 273-302.
Lekutai, G. (1997), "Adaptive self–tuning neuro wavelet network controllers", PhD Thesis; Electrical Engineering Department, Virginia Polytechnic Institute and State University.
Madandoust, R. and Mousavi, Y. (2012), "Fresh and hardened properties of self–compacting concrete containing metakaolin", *Constr. Build .Mater.*, **35**, 752-760.
Mahani, A.S., Shojaee, S., Salajegheh, E. and Khatibinia, M. (2015), "Hybridizing two–stage meta–heuristic optimization model with weighted least squares support vector machine for optimal shape of double–arch dams", *Appl. Soft. Comput.*, **27**, 205-218
Mirzaei, Z., Akbarpour, M., Khatibinia, M. and Khashei Siuki, A. (2015), "Optimal design of homogeneous earth dams by particle swarm optimization incorporating support vector machine approach", *Geomech. Eng.*, **9**(6), 709-727.
Mohseni, E., Sadat Hosseiny, S., Ranjbar, M.M., Roshandel, E. and Yazdi, M.A. (2015), "The effects of silicon dioxide, iron(III) oxide and copper oxide nanomaterials on the properties of self–compacting mortar containing fly ash", *Mag. Concrete. Res.*, **67**(20), 1112-1124.
Nazari, A. and Riahi, S. (2011a), "Effects of CuO nanoparticles on compressive strength of self-compacting concrete", *Sadhana*, **36**(3), 371-391.

Nazari, A. and Riahi, S. (2011b), "Effects of CuO nanoparticles on compressive strength of self-compacting concrete", *J. Indian. Acad. Sci.*, 371-391.

Niknam, T. and Farsani, E.A. (2010), "A hybrid self-adaptive particle swarm optimization and modified shuffled frog leaping algorithm for distribution feeder reconfiguration", *Eng. Appl. Artif. Intell.*, **23**(8), 1340-1349.

Oltulu, M. and Şahin, R. (2011), "Single and combined effects of nano-SiO_2, nano-Al_2 O_3 and nano-Fe_2 O_3 powders on compressive strength and capillary permeability of cement mortar containing silica fume", *Mater. Sci. Eng.: A*, **528**(22), 7012-7019.

Oltulu, M. and Şahin, R. (2013), "Effect of nano-SiO_2, nano-Al_2 O_3 and nano-Fe_2 O_3 powders on compressive strengths and capillary water absorption of cement mortar containing fly ash: a comparative study", *Ener. Build.*, **58**, 292-301.

Öztaş, A., Pala, M., Özbay, E., Kanca, E., Çagˇlar, N. and Bhatti, M.A. (2006), "Predicting the compressive strength and slump of high strength concrete using neural network", *Constr. Build. Mater.*, **20**(9), 769-775.

Park, D. and Rilett, L.R. (1999), "Forecasting freeway link travel times with a multilayer feedforward neural network", *Comput.-Aid. Civil and Infrastr. Eng.*, **14**(5), 357-367.

Park, Y.J. and Ang, A.H.S. (1985), "Mechanistic seismic damage model for reinforced concrete", *J. Struct. Eng.*, **111**(4), 722-739.

Quan, T., Liu, X. and Liu, Q. (2010), "Weighted least squares support vector machine local region method for nonlinear time series prediction", *Appl. Soft Comput.*, **10**(2), 562-566.

Ravi, V. (2008), "Advance in banking technology and management: impacts of ICT and CRM", Hershey, New York, NY, USA.

Sobhani, J., Khanzadi, M. and Movahedian, A.H. (2013), "Support vector machine for prediction of the compressive strength of no-slump concrete", *Comput. Concrete*, **11**(4), 337-350.

Sobolev, K., Flores, I., Torres-Martinez, L.M., Valdez, P.L., Zarazua, E. and Cuellar, E.L. (2009), "Engineering of SiO2 nanoparticles for optimal performance in nano cement-based materials", Nanotechnology in construction, **3**, 139-148, Springer Berlin Heidelberg.

Suykens, J.A., De Brabanter, J., Lukas, L. and Vandewalle, J. (2002), "Weighted least squares support vector machines: robustness and sparse approximation", *Neurocomput.*, **48**(1), 85-105.

Suykens, J.A.K., Brabanter, J.D., Lukas, L. and Vandewalle, J. (1999), "Least squares support vector machine classifiers", *Neural. Process. Lett.*, **9**(3), 293-300.

Topcu, I.B. and Sarıdemir, M. (2008), "Prediction of compressive strength of concrete containing fly ash using artificial neural network and fuzzy logic", *Comp. Mater. Sci.*, **41**(3), 305-311.

Vapnik, V. and Lerner, A. (1963), "Generalized portrait method for pattern recognition", *Automat. Rem. Contr.*, **24**(6), 774-780.

Wu, Q. (2010), "Product demand forecasts using wavelet kernel support vector machine and particle swarm optimization in manufacture system", *J. Comput. Appl. Math.*, **233**(10), 2481-2491.

Wu, Q. (2011), "Hybrid model based on wavelet support vector machine and modified genetic algorithm penalizing Gaussian noises for power load forecasts", *Exp. Syst. Appl.*, **38**(1), 379-385.

Yeh, I.C. (1998), "Modeling of strength of high–performance concrete using artificial neural networks", *Cem. Concr. Res.*, **28**(12), 1797-808.

Zavar, M., Rahati, S., Akbarzadeh-T, M.R. and Ghasemifard, H. (2011), "Evolutionary model selection in a wavelet-based support vector machine for automated seizure detection", *Exp. Syst. Appl.*, **38**(9), 10751-10758.